Modeling Flow and Transport in Saturated Fractured Rock to Evaluate Site Characterization Needs

Christine Doughty and Kenzi Karasaki

Earth Sciences Division
E.O. Lawrence Berkeley National Laboratory

Extended Abstract

Using regional geographic, geologic, hydrologic, geophysical, and meteorological data for the Tono area in Gifu, Japan, we developed an effective continuum model to simulate regional groundwater flow and the transport of radionuclides away from a hypothetical repository in a 4 km by 6 km by 3 km thick fractured granite rock mass overlain by sedimentary layers. Individual fractures are not modeled explicitly. Rather, continuum permeability and porosity distributions are assigned stochastically, based on well-test data and fracture density measurements. Large-scale features such as lithologic layering and major fault zones are assigned deterministically.

We start with a regular 3D grid with a basic grid block size of 100 m by 100 m by 100 m. Grid block thickness is decreased to 50 m near the top of the model, to enable better representation of surface topography changes. Grid block thickness is gradually increased near the bottom of the model since no data are available and flow variability is expected to be gradual at depth. The bottom of the model is a closed boundary. Next, we trim the grid laterally to reproduce the irregular 4 by 6 km model boundary that follows natural topographic boundaries such as ridgelines (closed boundaries) and rivers (open boundaries). Finally, we trim the grid vertically to match surface topography. The top of the model is held at a head value equal to the surface elevation, to represent a near-surface water table. Flow from the constant head boundary into the model represents subsurface recharge. This configuration eliminates the need to model percolation through the vadose zone, which is a highly non-linear process and hence computationally intensive.

We include the following features of interest deterministically:

- The Tsukiyoshi fault, a major east-west, subvertical fault is represented as a plane with location and orientation inferred from the surface trace, borehole occurrences, and seismic profiles. Several smaller surface lineaments identified from satellite or aerial images that are also identified in boreholes are modeled explicitly as well.

- Lithofacies changes observed in boreholes are kriged to form surfaces. These surfaces provide the boundaries between different material types in the model.

- The sediment/bedrock boundary inferred from an electrical resistivity survey is used as the boundary between the uppermost granite (Biotite) and the lowermost sedimentary rock (Toki-lignite bearing rock).

The resulting model is shown in Figure 1 and Table 1 summarizes the various types of surface and subsurface data used to construct it.

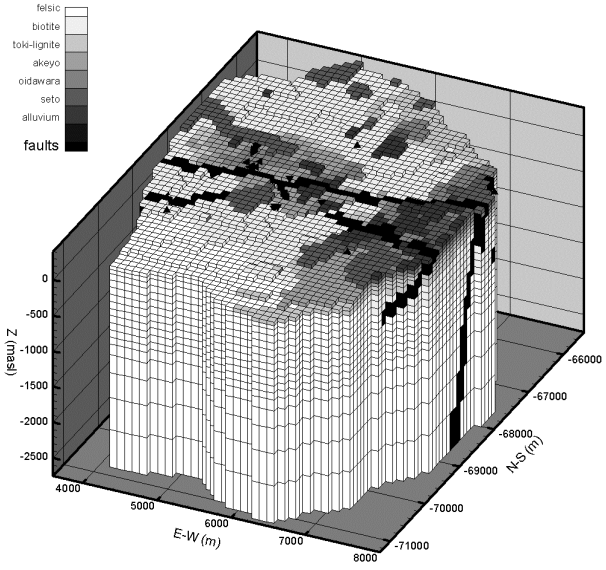

Figure 1. 3D perspective view of the model.

Table 1. Summary of data used to develop the 4x6 km model.

Data Type	Actual Use	Potential Use
Landsat images	Qualitative understanding of regional surface topography	Improve lateral model boundaries at great depths
Surface topography	Provide detailed topography that impacts shallow groundwater flow	
Seismic profiles	Locate faults in 2-D sections	
Electrical resistance	Provide spatially extensive image of the sediment/bedrock boundary	
Surface geological map	Verify granite outcrop locations in model	Improve assignment of shallow material types, especially among sedimentary rocks
Water balance data	Estimate average surface recharge into the model	Identify locations of especially large or small recharge
Wellbore lithologies	Assign material types	
Wellbore fracture identification	Determine stochastic distribution of fracture density for use in calculation of model porosity	
Well tests	Provide distributions of conductivity values for model	Use in inversion to determine conductivity of specific regions
Multi-packer monitoring	Investigate connectivity and flow barriers	Same as well tests
Drillers' notes		Identify high flow zones
Flow and temperature logs		Investigate regional groundwater flow

Each grid block represents an effective fractured continuum with permeability and porosity assigned stochastically based on field measurements. Permeability is proportional to hydraulic conductivity K, which is determined from slug tests and pumping tests conducted using packed-off intervals in boreholes. Because many of the intervals used for the tests are of the same order as the grid block size, we assume that there is no need to scale up or scale down K values measured during well tests, and that they directly represent effective continuum conductivities. Grid block K values are drawn from random distributions for each material type, constructed by resampling field measurements, unless there are not enough measurements for a given material type to make resampling viable, in which case a log-normal distribution is used. Table 2 summarizes the material types and conductivity distributions used for the model.

Porosity ϕ is calculated as the product of fracture aperture w and fracture density d, with aperture determined from K and d using the cubic law:

$$\phi = w\, d = (12\, K\, \mu / d)^{1/3}\, d = (12\, K\, \mu\, d^2)^{1/3}. \quad (1)$$

Fracture density measurements are sparse and there is no obvious correlation between fracture density and conductivity, so fracture density measurements from all lithological layers are combined to determine a mean fracture density of 7.95 m^{-1} and a standard deviation of 5 m^{-1}. For most of the lithological layers, fracture densities are drawn from a normal distribution with these moments, which is truncated at a small positive number (0.01 m^{-1}) to ensure that fracture density is always positive.

For each grid block, after K and d have been drawn from the appropriate distribution, Equation (1) is applied to determine ϕ. The resulting model porosity statistics are summarized in Table 2. Model porosity is considered to be less well constrained than model conductivity for several reasons. First, basing porosity estimates on fracture density measurements is problematic because a high percentage of observed

Table 2. Summary of material properties used in the model. For materials with no data, use average for all materials.

Material Type	Number. of conductivity measurements	$Log_{10}K$ (m/s)		Type of distribution used for $log_{10}K$	
		Mean	S.D.		
Alluvium	0	–7.9	1.6	Normal	
Seto group	0	–7.9	1.6	Normal	
Oidawara	1	–8.7	1.6	Normal	
Akeyo	11	–7.9	0.8	Resampled	
Toki lignite-bearing	21	–7.0	0.9	Resampled	
Biotite granite	192	–7.1	1.7	Resampled	
Felsic granite	46	–6.9	1.1	Resampled	
Faults	12	–7.7	1.0	Tsukiyoshi resampled; other faults normal	
Material Type	Number. of fracture density measurements	Fracture density (m^{-1})		Model Porosity	
		Mean	S.D.	Mean	S.D.
Biotite granite	57	7.7	4.2	3.9E-4	5.9E-4
Felsic granite	4	10.8	4.2	3.5E-4	2.7E-4
Overall	67	7.9	5.0	3.2E-4	4.2E-4

fractures may not contribute to flow at all. Moreover, the cubic law can greatly misrepresent the relationship between fracture aperture and conductivity, and even if it is valid, the hydraulic aperture used in the cubic law tends to underestimate the volumetric aperture relevant for transport. Finally, there are very few fracture density measurements available for materials other than the Biotite granite.

The numerical simulator TOUGH2 simulates the steady-state groundwater flow through the site, then streamline tracing analysis is used to calculate travel times to the model boundary from specified monitoring points that represent leakage from a hypothetical nuclear waste repository. These travel times consider transport due to advection only; no diffusion or dispersion is included.

The base case simulation was conducted for 10 realizations of the stochastic permeability and porosity distributions. For all realizations, the modeled water balance is reasonable, with the modeled recharge about a factor of two smaller than the value inferred from rainfall, evaporation, and streamflow data. Most of the outflow is to or below the Toki River, which constitutes the southern boundary of the model. Predicted travel times from the repository site to the model boundaries range from 1 to 25 years, with a mean of 7 years.

Observed heads above and below the Tsukiyoshi fault suggest that it may act as a low-permeability barrier to flow. To test this hypothesis, we consider a case in which the permeability of grid blocks representing the Tsukiyoshi fault is decreased by a factor of ten. Figure 2 shows head profiles for several realizations of the two cases. The effect of assigning lower permeability to the Tsukiyoshi fault results in an obvious increase in head below the fault depth that is consistent with field observations. In addition, the average travel time increases slightly, from 7 to 9 years.

There is significant variability among the different stochastic realizations in terms of the details of the streamtrace patterns, including model exit locations. However, if only average results such as the mean travel time or mean path length are considered, then variability among realizations is relatively small. Greater variability arises from imposing different boundary conditions or assigning low permeabilities to the Tsukiyoshi fault, emphasizing the need to establish a sound basis for determining these model properties.

Several other research groups also developed models based on the same data set, and a key feature of the work is a comparison between different models' results to highlight which aspects of site characterization need to be improved in order to increase confidence in model predictions. Because a field investigation program is ongoing, model results can potentially have a significant impact on future characterization activities. The effective porosity of the fracture network is the least well-constrained parameter of our model, and a wide range in travel times obtained by the different research groups (1 to 1,000,000 years) can be attributed to orders of magnitude differences in the effective porosities used. This underscores the importance of improved porosity estimates as a key component of future site characterization.

This work was supported by Japan Nuclear Fuel Cycle Corporation (JNC) and Taisei Corporation of Japan. through the U.S. Department of Energy Contract No. DE-AC03-76SF00098.

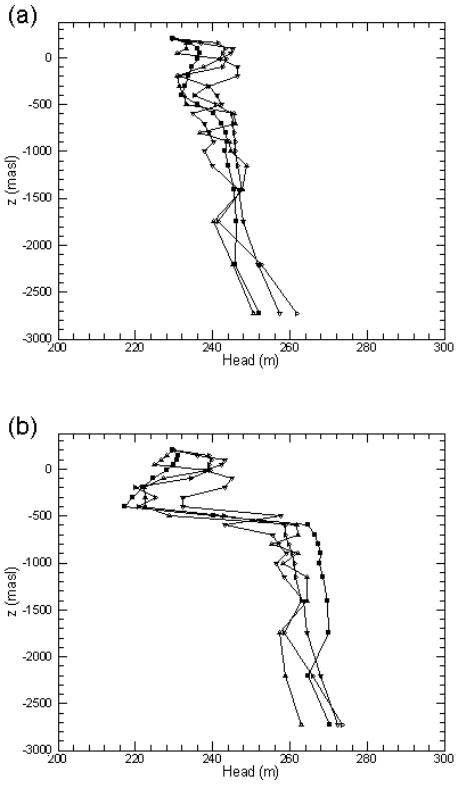

Figure 2. Head profiles for (a) the base case; and (b) the low-permeability Tsukiyoshi fault case.